Development of preoperative and postoperative machine learning models to predict the recurrence of huge hepatocellular carcinoma following surgical resection

QINGHUA ZHANG[1*], GUOXU FANG[2,3*], TIANCONG HUANG[4*], GUANGYA WEI[1], HAITAO LI[2] and JINGFENG LIU[3,5]

[1]Department of Hepatobiliary Pancreatic Cancer Surgery, College of Clinical Medicine for Oncology, Fujian Medical University, Fuzhou, Fujian 350108; [2]Department of Hepatopancreatobiliary Surgery, Mengchao Hepatobiliary Hospital of Fujian Medical University; [3]The Big Data Institute of Southeast Hepatobiliary Health Information, Mengchao Hepatobiliary Hospital of Fujian Medical University, Fuzhou, Fujian 350025; [4]Department of Hepatopancreatobiliary Surgery, The Second Affiliated Hospital of Fujian Medical University, Quanzhou, Fujian 362000; [5]Department of Hepatopancreatobiliary Surgery, Clinical Oncology School of Fujian Medical University, Fujian Cancer Hospital, Fuzhou, Fujian 350014, P.R. China

Received January 3, 2023; Accepted April 5, 2023

DOI: 10.3892/ol.2023.13861

Abstract. Resection has been commonly utilized for treating huge hepatocellular carcinoma (HCC) with a diameter of ≥10 cm; however, a high rate of mortality is reported due to recurrence. The present study was designed to predict the recurrence following resection based on preoperative and postoperative machine learning models. In total, 1,082 patients with HCC who underwent liver resection in the Eastern Hepatobiliary Surgery Hospital cohort between January 2008 and December 2016 were divided into a training cohort and an internal validation cohort. In addition, 164 patients from Mengchao Hepatobiliary Hospital cohort between January 2014 and December 2016 served as an external validation cohort. The demographic information, and serological, MRI, and pathological data were obtained from each patient prior to and following surgery, followed by evaluating the model performance using the concordance index, time-dependent receiver operating characteristic curves, prediction error cures, and a calibration curve. A preoperative random survival forest (RSF) model and a postoperative RSF model were constructed based on the training set, which outperformed the conventional models, such as the Barcelona Clinic Liver Cancer (BCLC), the 8th edition of the American Joint Committee on Cancer (AJCC 8th) staging systems, and the Chinese stage systems. In addition, the preoperative and postoperative RSF models could also re-stratify patients with BCLC stage A/B/C or AJCC 8th stage IB/II/IIIA/IIIB or Chinese stage IB/IIA/IIB/IIIA into low-risk, intermediate-risk, and high-risk groups in the training and the two validation cohorts. The preoperative and postoperative RSF models were effective for predicting recurrence in patients with huge HCC following hepatectomy.

Correspondence to: Dr Jingfeng Liu, Department of Hepatopancreatobiliary Surgery, Clinical Oncology School of Fujian Medical University, Fujian Cancer Hospital, 420 Fuma Road, Fuzhou, Fujian 350014, P.R. China
E-mail: drjingfeng@126.com

Dr Haitao Li, Department of Hepatopancreatobiliary Surgery, Mengchao Hepatobiliary Hospital of Fujian Medical University, 312 Xihong Road, Fuzhou, Fujian 350025, P.R. China
E-mail: lht45182@163.com

*Contributed equally

Key words: huge hepatocellular carcinoma, liver resection, recurrence, machine learning, individualized prediction

Introduction

Hepatocellular carcinoma (HCC) is one of the most common types of cancer worldwide and is the second leading cause of cancer-related death (1). As the symptoms are usually insidious, the majority of the patients present with advanced-stage HCC upon diagnosis. Furthermore, certain patients possess a huge tumor with a size of ≥10 cm upon diagnosis, resulting in a poor prognosis even after treatment (2). For patients presenting with resectable HCC with well-preserved liver function, hepatectomy is preferred for treatment; however, the outcomes are compromised due to a postoperative recurrence rate of 60-70% within 5 years (3-5).

Hepatectomy is the preferred option for treating huge HCC. However, the outcome following hepatectomy remains unsatisfactory as the R0 resection rate is still <20% (6). To date, alternative choices exist for patients in whom hepatectomy is not recommended, such as transarterial chemoembolization (TACE), hepatic artery infusion chemotherapy, radiofrequency ablation, and sorafenib or Lenvatinib (7). Therefore, a proper preoperative prognostic prediction is essential for the selection of the optimal regimen.

The COX proportional hazard (CPH) model has been commonly utilized in evaluating prognosis by predicting the

recurrence rate based on the prognostic factors (8-10). However, its predictive performance is limited as it cannot model the complicated, multidimensional, and non-linear relationships among different prognostic variables. Therefore, there is an urgent need to develop novel solutions for accurate prognostic prediction even if it involves non-linear variables. Recently, additional attention has been paid to machine learning, in which machines mimic, recognize, and learn cognitive functions of the human mind for performing empirical predictions (11). The random survival forest (RSF) model is a non-parametric machine-learning strategy that can be utilized for the prediction of survival analysis among patients with cancer (12). RSF is superior to CPH models as it uses non-linear functions and considers all possible interactions between variables to improve the predictive performance (13). Moreover, the RSF model is superior to the conventional regression models in predicting the prognosis of HCC (14). In the present study, the preoperative and postoperative risk factors for the recurrence of huge HCC were investigated. A preoperative and postoperative RSF model for predicting the recurrence of huge HCC was constructed. The following article/case is presented in accordance with the STROBE reporting checklist (15).

Materials and methods

Patients and study design. The data of 1,192 consecutive patients [male, 934, median age: 48.31±11.26 (IQR, 18-79); female: 258, median age: 49.35±12.56 (IQR, 21-89 years)] who underwent liver resection for huge HCC at the Eastern Hepatobiliary Surgery Hospital (EHSH) between January 2008 and December 2016 and at the Mengchao Hepatobiliary Hospital (MHH) between January 2014 and December 2016 were retrospectively reviewed. HCC was diagnosed according to the practice guidelines recommended by the American Association for the Study of Liver Diseases (16). The patients with the following conditions were included in the present study: i) Those confirmed to have HCC by immunohistochemistry, presenting an HCC lesion with a diameter ≥10 cm; ii) Child-Pugh A or B liver function; iii) absence of extra-hepatic metastasis; and iv) with R0 resection, defined as complete resection of macroscopic tumor nodules with tumor-free margins confirmed by histological examination. Patients with the following conditions were excluded from the present study: i) Those who received palliative tumor resection; ii) those who underwent preoperative anticancer treatments; iii) those with a history of other malignancies; or iv) those with incomplete clinical data and those lost to follow-up within 2 months following hepatectomy.

All data in the present study were verified by three independent researchers. To establish the RSF model, qualified patients from the EHSH were randomly assigned to the training cohort and the internal validation cohort with a 7:3 ratio. All qualified patients from the MHH served as the external validation cohort. The protocol of the present study was granted approval from the Medical Ethics Committee of Mengchao Hepatobiliary Hospital of Fujian Medical University (2022-027-01). Written informed consent for participation was not required for this study in accordance with national legislation and institutional requirements.

Preoperative assessment. All patients underwent routine preoperative examinations, including immunology of hepatitis B virus and hepatitis C viral infection, α-fetoprotein (AFP) concentration, prothrombin time (PT), activated partial thromboplastin time (APTT), fibrinogen (Fg) concentration, white blood cell count, platelet (PLT), and liver and kidney function examination. In addition, imaging examination was provided to each patient including chest X-ray, abdominal ultrasound, contrast-enhanced CT scan, and/or MRI of the abdomen.

Surgical procedures. The decision of anatomical or partial hepatectomy is commonly based on liver function, tumor number, and location. Specifically, anatomical hepatectomy was preferentially given to patients with a well-preserved liver function and tumors located within a segment, sector, and hemiliver. Partial hepatectomy was provided to patients with poor liver function. For huge HCC, the anterior approach was often used for hepatectomy. Specifically, the liver was transected along the principle plane dividing the right from the left hemiliver, with or without hepatic inflow clamping, to the anterior of the inferior vena cava. The corresponding hepatic pedicle, hepatic vein, and short hepatic veins were ligated. Finally, the liver ligaments were freed to remove the hemiliver harboring the tumor. Intraoperative liver ultrasonography was routinely performed to ensure the complete resection of detectable tumors, followed by pathological analysis.

End points and follow-up. The end points of the study included overall survival (OS) and recurrence-free survival (RFS). OS was defined as the interval between the date of surgery and the date of death or loss to follow-up. RFS was defined as the interval between the date of surgery and the date of recurrence. Each patient was followed up based on the conventional program and the recurrence was confirmed according to the criteria previously described (17).

RSF modeling process. The RSF model was applied to real data settings to uncover highly complex interrelationships between variables; it can also estimate the individual cumulative hazard function by integrating the Nelson-Allen estimator in the model (18,19). Variable Importance (VIMP) was obtained by measuring the decrease in prediction accuracy using out-of-bag data which were not used for building trees each time. The variables were selected by filtering based on their VIMP. The risk index was derived from the estimated cumulative hazard function. The Cox model involved a continuous covariate and was utilized to evaluate the significance of the risk index. The risk groups were generated by the 50th and 85th percentile of the risk index (20). Kaplan-Meier curves for each risk group were plotted in each cohort.

The RSF model was constructed based on the results of the VIMP of recurrence in the training cohort. The preoperative and postoperative RSF model was established based on the preoperative clinical imaging data and the clinicopathological variables, respectively. The predictive performance of the RSF model was measured using Harrell's concordance index (C-index), the time-dependent areas under the receiver operating characteristic curve (tdAUC), the prediction error curve, and the calibration plot (21,22). Clinical usefulness was measured by decision curve analysis (DCA) with a net benefit at a threshold of 50%. The overall performance was measured by the prediction error curves. The cumulative

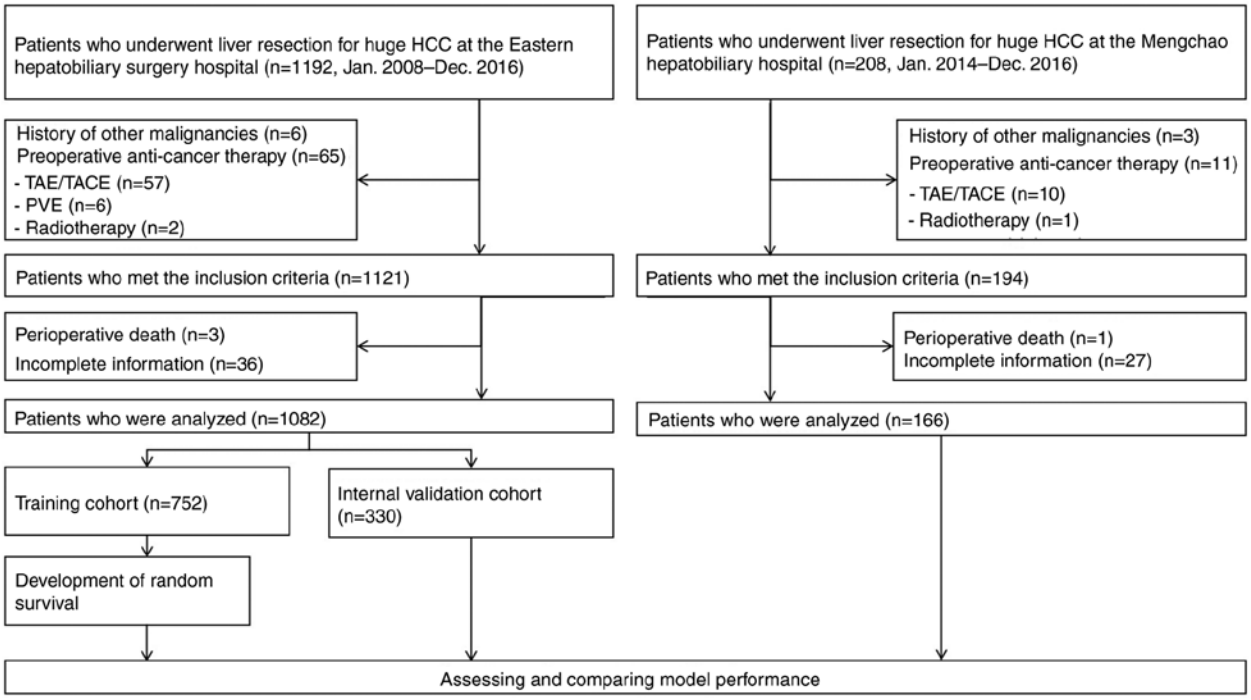

Figure 1. Flowchart for establishment of the three cohorts in this study.

recurrence between each risk group was assessed and tested using Kaplan-Meier curves and the log-rank test, respectively. The discrimination of the RSF model was also compared with the AJCC TNM stage (23), Barcelona Clinic Liver Cancer (BCLC) stage (24), and Chinese stage (25) in each cohort.

Statistical analysis. Statistical analyses were performed using SPSS version 22.0, R version R-4.2.3 (r-project.org/) and R studio (4.2 version, rstudio.com/). The categorical variables are presented as the frequency and percentage, and continuous variables are presented as the mean ± standard error. A χ^2 test or Fisher's exact test was used for the inter-group comparisons of the categorical variables. A Student's t-test or a Mann-Whitney U test was used for the comparison of the continuous variables. Kaplan-Meier analysis was used to estimate the cumulative rates of survival. The comparison of the survival curves was performed based on a log-rank test. The continuous variables not normally distributed were presented as the median or interquartile range and were compared using a Mann-Whitney U test. All statistical tests were two-tailed. $P<0.05$ was considered to indicate a statistically significant difference.

Results

Participant characteristics. In total, 1,192 consecutive patients (male: 934; female: 258) underwent partial hepatectomy for huge HCC at EHSH between January 2008 and December 2016. A total of 110 patients were excluded due to preoperative anticancer therapy (n=65), history of other malignancies (n=6), incomplete information (n=36), and perioperative death (n=3). Finally, 1,082 patients were included and randomly divided into a training cohort (n=752) and a validation cohort (n=330) based on a ratio of 7:3. For the external validation cohort, 208 patients from MHH between January 2014 and December 2016, and finally 166 patients met the inclusion criteria following exclusion of the history of malignancies (n=3), preoperative anticancer therapy (n=11), incomplete information (n=27), and perioperative death (n=1). The flowchart of this process is shown in Fig. 1.

The baseline clinicopathological features of the participants are listed in Table I. No statistical differences were noted in the baseline clinicopathological characteristics between the training and the internal validation cohorts (Table I). In contrast to these observations, several clinicopathological features did differ amongst the training, internal, and external cohorts, including PT, APTT, Fg, tumor capsular, microvascular invasion (MVI), and Edmondson-Steiner grade ($P<0.01$).

Prognosis. The study was censored on December 31, 2021, for the training and internal validation cohorts. The median follow-up period was 31.41 (range, 2-143) months and 25.94 (range, 2-97) months in the training and internal validation cohorts. The 1-, 3-, and 5-year OS rates in the training cohort were 84, 59.1, and 45.8%, and the 1-, 3-, and 5-year RFS rates were 69.2, 44.1, and 23.7%, respectively (Table II). In the internal validation cohort, the median survival was 41.6 months (range, 2-97) months. The 1-, 3-, and 5-year OS rates in the internal validation cohort were 80.78, 55.4, and 43.55%, while the 1-, 3-, and 5-year RFS rates were 69.3, 45.2, and 29.7%, respectively. The last follow-up for patients in the external validation cohort was on December 31, 2021. The median survival of these patients was 25.06 (range, 2-84) months. In the external validation cohort, the 1-, 3-, and 5-year OS rates were 78.75, 52.38, and 38.26%, respectively; in the same cohorts, the 1-, 3-, and 5-year RFS rates were 60.5, 39.8, and 29.2%, respectively. No significant differences were noted among these three cohorts in the 1-, 3-, and 5-year OS

Table I. Clinicopathologic features.

Variable	Training cohort, n=752	Internal cohort, n=330	External cohort, n=164	P-value[d]	P-value[e]
Age, Mean (SD), years	47.9 (11.4)	49.2 (10.9)	48.9 (11.4)	0.066	0.282
Sex, n (%)				0.783	0.446
Female	102 (13.6%)	42 (12.7%)	26 (15.9%)		
Male	650 (86.4%)	288 (87.3%)	138 (84.1%)		
Etiology, n (%)				0.237	0.292
HBV	564 (75.0%)	263 (79.7%)	133 (81.1%)		
HCV	2 (0.3%)	1 (0.3%)	1 (0.6%)		
Others	186 (24.7%)	66 (20.0%)	30 (18.3%)		
ALB, Mean (SD), g/l	40.7 (3.92)	40.3 (3.47)	38.4 (3.94)	0.08	0.003[b]
Mean TBIL (SD), μmol/l	14.7 (11.6)	13.9 (5.58)	15.4 (7.0)	0.126	0.141
AST, Mean (SD), U/l	50.0 (23.3)	49.8 (22.2)	60.1(48.3)	0.922	0.009[b]
PT (s), Mean (SD)	12.4 (4.38)	12.3 (1.43)	13.1 (1.28)	0.662	<0.001[c]
APTT (s), Mean (SD)	27.9 (4.26)	27.5 (3.95)	33.5 (6.66)	0.122	<0.001[c]
Fg, (mg/dl), Mean (SD)	3.07 (0.923)	3.03 (0.903)	3.59 (1.02)	0.529	<0.001[c]
AFP (ng/ml), Median (IQR)	920 (21.9-1210)	531 (21.6-1,210)	761 (43.3-1,210)	0.313	0.157
Neutrophil Count, Mean (SD), x10^9/l	3.85 (1.55)	3.68 (1.36)	4.16 (1.71)	0.074	0.012[a]
Lymphocyte Count, Mean (SD), x10^9/l	1.51 (0.536)	1.55 (0.57)	1.48 (0.483)	0.331	0.277
Mean platelets (SD), x10^9/l	197 (84.8)	200 (82.4)	209 (92.9)	0.558	0.141
PLR, Mean (SD)	139. 76 (69.1)	143.54 (74.48)	150.98 (74.97)	0.622	0.162
PNLR, Mean (SD)	564.14 (426.08)	545.50 (416.96)	645.14 (424.74)	0.483	0.016[a]
Tumor number, n (%)				0.362	0.157
1	547 (72.7%)	249 (75.5%)	120 (73.2%)		
2	96 (12.8%)	38 (11.5%)	25 (15.2%)		
3	31 (4.1%)	7 (2.1%)	9 (5.5%)		
≥4	78 (10.4%)	36 (10.9%)	10 (6.1%)		
Mean tumor size (SD), cm	13.34 (2.65)	13.6 (2.69)	13.27 (2.58)	0.152	0.462
Tumor number[f], n (%)				0.415	0.121
1	547 (72.7%)	249 (75.5%)	120 (73.2%)		
2	100 (13.3%)	40 (12.1%)	25 (15.2%)		
3	27 (3.6%)	6 (1.8%)	9 (5.5%)		
≥4	78 (10.4%)	35 (10.6%)	10 (6.1%)		
Tumor size[f], Mean (SD), cm	13.28 (2.57)	13.46 (2.52)	13.2 (2.48)	0.282	0.526
Satellite nodules, n (%)				0.0554	0.08
Present	416 (55.3%)	161 (48.8%)	100 (61.0%)		
Absent	336 (44.7%)	169 (51.2%)	64 (39.0%)		
Tumor capsule, n (%)				0.253	<0.001[c]
Complete	214 (28.5%)	106 (32.1%)	20 (12.2%)		
Incomplete	538 (71.5%)	224 (67.9%)	144 (87.8%)		
Cirrhosis, n (%)	539 (71.7%)	238 (72.1%)	109 (66.5%)	0.939	0.188
Macrovascular invasion, n (%)	114 (15.2%)	45 (13.6%)	31 (18.9%)	0.577	0.2
Macrovascular invasion[f], n (%)	110 (14.6%)	43 (13.0%)	30 (18.3%)	0.549	0.2
Microvascular invasion, n (%)	345 (45.9%)	154 (46.7%)	125 (76.2%)	0.862	<0.001[c]
Edmondson-Steiner classification, n (%)				0.937	<0.001[c]
I-II	34 (4.5%)	16 (4.8%)	31 (18.9%)		
III-IV	718 (95.5%)	314 (95.2%)	133 (81.1%)		
Intraoperative blood transfusion, n (%)				0.993	0.812
Yes	175 (23.3%)	76 (23.0%)	40 (24.4%)		
No	577 (76.7%)	254 (77.0%)	124 (75.6%)		
BCLC staging system, n (%)				0.787	0.181
A	470 (62.5%)	225 (68.2%)	99 (60.4%)		

Table I. Continued.

Variable	Training cohort, n=752	Internal cohort, n=330	External cohort, n=164	P-value[d]	P-value[e]
B	168 (22.3%)	73 (22.1%)	34 (20.7%)		
C	114 (15.2%)	32 (9.7%)	31 (18.9%)		
AJCC staging system[8th], n (%)				0.559	<0.001[c]
Ib	312 (41.5%)	133 (40.3%)	37 (22.6%)		
II	158 (21.0%)	92 (27.9%)	68 (41.5%)		
IIIa	168 (22.3%)	73 (22.1%)	28 (17.1%)		
IIIb	114 (15.2%)	32 (9.7%)	31 (18.9%)		
Chinese staging system, n (%)				0.077	0.027[a]
Ib	470 (62.5%)	225 (68.2%)	99 (60.4%)		
IIa	99 (13.2%)	39 (11.8%)	27 (16.5%)		
IIb	69 (9.2%)	34 (10.3%)	7 (4.3%)		
IIIa	114 (15.2%)	32 (9.7%)	31 (18.9%)		

[a]P<0.05, [b]P<0.01, [c]P<0.001. [d]Comparison between the training cohort and the internal validation cohort from EHSH. [e]Comparison between the external validation cohort from Mengchao Hepatobiliary Hospital and all patients in the training and internal validation cohorts from EHSH. [f]Preoperative images were obtained from contrast-enhanced Computed Tomography or contrast-enhanced magnetic resonance imaging. HBV, hepatitis B virus; HCV, hepatitis C virus; ALB, Albumin; TBIL, total bilirubin; AST, aspartate aminotransferase; PT, prothrombin time; APTT, activated partial thromboplastin time; Fg, fibrinogen; AFP, alpha fetoprotein; PLR, platelet-to-lymphocyte ratio; BCLC, Barcelona Clinic Liver Cancer staging system; AJCC, American Joint Committee on Cancer; SD, standard deviation; IQR, interquartile range; EHSH, Eastern Hepatobiliary Surgery Hospital.

Table II. Prognosis of training cohort, internal validation cohort, and external validation cohort.

Survival	Cohort	1-year	3-years	5-years	P-value
Overall survival					0.117
	Training set	0.8400	0.5910	0.4580	
	Internal validation	0.8078	0.5540	0.4355	
	External validation	0.7875	0.5238	0.3826	
Recurrence-free survival					0.052
	Training set	0.6920	0.4410	0.2370	
	Internal validation	0.6930	0.4520	0.2970	
	External validation	0.6050	0.3980	0.2920	

and RFS rates following liver resection (P=0.117 and 0.052, respectively).

Preoperative and postoperative RSF models for predicting recurrence. The common variables used for preoperative and postoperative analyses were the demographic data, including age, sex, HCC family history, preoperative serological data, imaging data, and platelet-to-lymphocyte ratio (PLR) as listed in Table I. The preoperative modeling was based on the MRI findings, while the postoperative modeling was conducted based on the pathological results. Finally, the preoperative RSF model was constructed using 16 features. The prediction error rate was low and stable during the process of constructing 1,000 survival trees (Fig. 2A); subsequently, the VIMP for all the features used for growing the trees was generated. The top 10 variables were macrovascular invasion (MaVI), satellite nodules, tumor number, age, AFP, aspartate aminotransferase, fibrinogen, platelet neutrophil/lymphocyte ratio (PNLR), PLR, and PT. Postoperatively, the RSF model was constructed using 21 features and the top 10 variables were MaVI, satellite nodules, tumor number, age, AFP, fibrinogen, aspartate aminotransferase, PNLR, PLR, and PT (Fig. 2B).

Efficiency of the preoperative and postoperative RSF model in recurrence prediction. Both preoperative and postoperative RSF models of the training, internal, and external validation cohorts could feasibly predict the recurrence of HCC following surgery. The C-index of the preoperative RSF model in the training, internal validation, and external validation cohorts was 0.766 (95% CI: 0.749-0.785), 0.745 (95% CI: 0.726-0.764), and 0.731 (95% CI: 0.713-0.749), respectively. The Gönen & Heller's K values of the preoperative RSF model were 0.699

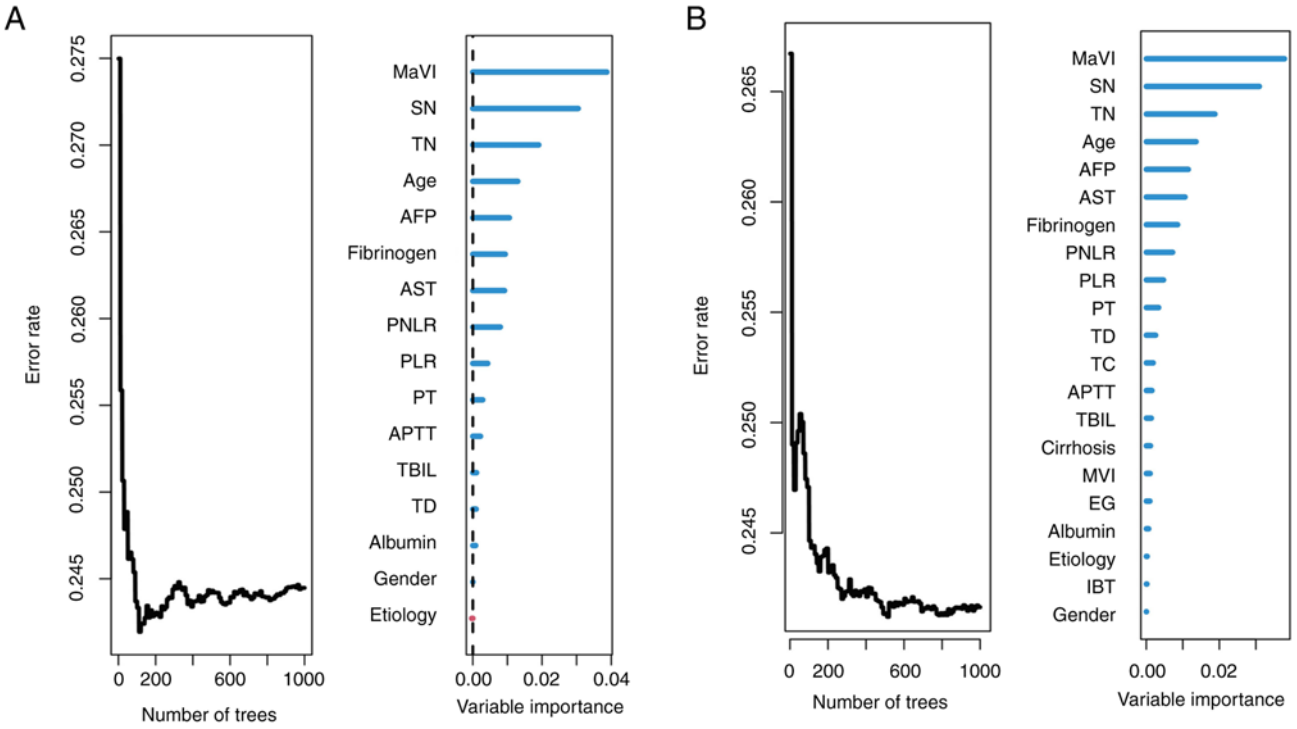

Figure 2. Construction of the preoperative RSF model and postoperative RSF model for prediction of recurrence in the training cohort. (A) preoperative RSF model, (B) postoperative RSF model. RSF, random survival forests; SN, satellite nodules; AST, aspartate aminotransferase; AFP, α-fetoprotein; TN, tumor number; PNLR, platelet-neutrophil-lymphocyte ratio; MaVI, macrovascular invasion; TD, tumor diameter; PT, prothrombin time; PLR, platelet-to-lymphocyte ratio; APTT, activated partial thromboplastin time; HCVAb, hepatitis C virus antibody; HBsAg, hepatitis B virus surface antigen; EG, Edmondson-Steiner classification; TC, tumor capsule; IBT, intraoperative blood transfusion; ALT, aspartate aminotransferase; MVI, microvascular invasion; AFP, α fetoprotein; ALB, albumin; PLT, platelet count; TBIL, total bilirubin.

(95% CI: 0.681-0.717), 0.695 (95% CI: 0.666-0.724), and 0.683 (95% CI: 0.638-0.728), respectively. The recurrence prediction of the preoperative RSF model in the three cohorts was significantly improved compared with that obtained based on the 8th edition of the AJCC TNM stage (23), BCLC stage (24), and Chinese stage (25) (Table III).

For the postoperative RSF model, the C-index values were 0.775 (95% CI: 0.756-0.794) in the training cohort, 0.746 (95% CI: 0.727-0.765) in the internal validation cohort, and 0.758 (95% CI: 0.739-0.777) in the external validation cohort, respectively. The Gönen & Heller's K values of the postoperative RSF model were 0.704 (95% CI: 0.688-0.719), 0.693 (95% CI: 0.664-0.722), and 0.696 (95% CI: 0.655-0.737), respectively. The recurrence prediction of the postoperative RSF model was improved compared with that of the BCLC stage, the 8th edition of the AJCC stage, and the Chinese staging systems, together with the time-dependent Brier score and R2 (Table III).

Time-dependent receiver operating characteristic curve analysis was also performed to assess the discriminative efficiency of the RSF model. For the preoperative RSF model, the median time dependent AUCs of the RSF model were 0.784 (95% CI: 0.725-0.813) in the training cohort, 0.778 (95% CI: 0.745-0.809) in the internal validation cohort, and 0.74 (95% CI: 0.702-0.801) in the external validation. For the postoperative RSF model, the corresponding tdAUC was 0.793 (95% CI: 0.742-0.825) in the training cohort, 0.777 (95% CI: 0.745-0.813) in the internal validation cohort, and 0.774 (95% CI: 0.732-0.828) in the external validation cohort, respectively. Both models had higher tdAUCs than those of the BCLC, AJCC, and Chinese staging systems (Fig. 3A and C).

DCA was used to compare the predictive performance of the preoperative and postoperative RSF models with BCLC, AJCC, and Chinese staging system-based models in the three cohorts. The net benefit of the RSF models was superior to that of the other models as revealed by DCA (Fig. 4A-C). The prediction error curve analysis was used to assess the overall predictive performance of the RSF models. The RSF models had a lower prediction error rate than those of the conventional staging systems (Fig. 5A and C). An optimal consistency was noted between the calibration plots of the preoperative and postoperative RSF models. In addition, the probabilities of 1-, 3-, and 5-year recurrence in the training and validation cohorts were also consistent (Fig. 6).

Risk stratification based on the RSF score. For the risk stratification, the patients were stratified into three subgroups including low-risk, intermediate-risk, and high-risk groups based on the cut-off points that corresponded to the 50th (29.377) and 85th (58.741) percentile of the risk index in the training cohort of the preoperative and postoperative RSF models (50th percentile: 29.692; 85th percentile: 59.183). The model exhibited optimal discriminative ability for recurrence in the presence of apparent distinction from the recurrence curves of the subgroups based on Kaplan-Meier analysis (Fig. 7). To facilitate the clinical application, two web-based prediction tools (https://preoperative-prediction.shinyapps.io/pre-operative_predict/; and https://preoperative-prediction.

Table III. Prognostic performance of the pre- and postoperative random survival forests model.

Measure of discrimination	Cohort	RSF-preoperative (SE)	RSF-postoperative (SE)	BCLC (SE)	AJCC TNM (SE)	Chinese staging system (SE)
Harrell's c-index	Training set	0.766 (0.097)	0.775 (0.097)	0.665 (0.097)	0.663 (0.097)	0.671 (0.097)
	Internal validation	0.745 (0.095)	0.746 (0.095)	0.634 (0.095)	0.645 (0.095)	0.639 (0.095)
	External validation	0.731 (0.094)	0.758 (0.095)	0.632 (0.094)	0.574 (0.094)	0.631 (0.094)
tdAUC (5 years)	Training set	0.784 (0.028)	0.793 (0.028)	0.671 (0.027)	0.676 (0.029)	0.677 (0.027)
	Internal validation	0.774 (0.041)	0.778 (0.041)	0.634 (0.042)	0.671 (0.047)	0.631 (0.045)
	External validation	0.740 (0.065)	0.774 (0.062)	0.651 (0.056)	0.624 (0.061)	0.649 (0.056)
Gönen & Heller's K	Training set	0.699 (0.009)	0.704 (0.008)	0.622 (0.008)	0.643 (0.011)	0.624 (0.008)
	Internal validation	0.695 (0.015)	0.693 (0.015)	0.606 (0.014)	0.639 (0.017)	0.606 (0.014)
	External validation	0.683 (0.023)	0.696 (0.021)	0.603 (0.021)	0.588(0.027)	0.595(0.021)
Royston-Sauerbrei's R^2	Training set	0.184	0.205	0.067	0.047	0.061
	Internal validation	0.218	0.266	0.103	0.034	0.028
	External validation	0.251	0.256	0.071	0.112	0.102
Time-dependent Brier (5 years)	Training set	0.189	0.184	0.228	0.228	0.226
	Internal validation	0.192	0.185	0.221	0.231	0.230
	External validation	0.186	0.179	0.221	0.217	0.217

BCLC, Barcelona Clinic Liver Cancer staging system; AJCC, American Joint Committee on Cancer Tumor-Node-Metastasis.

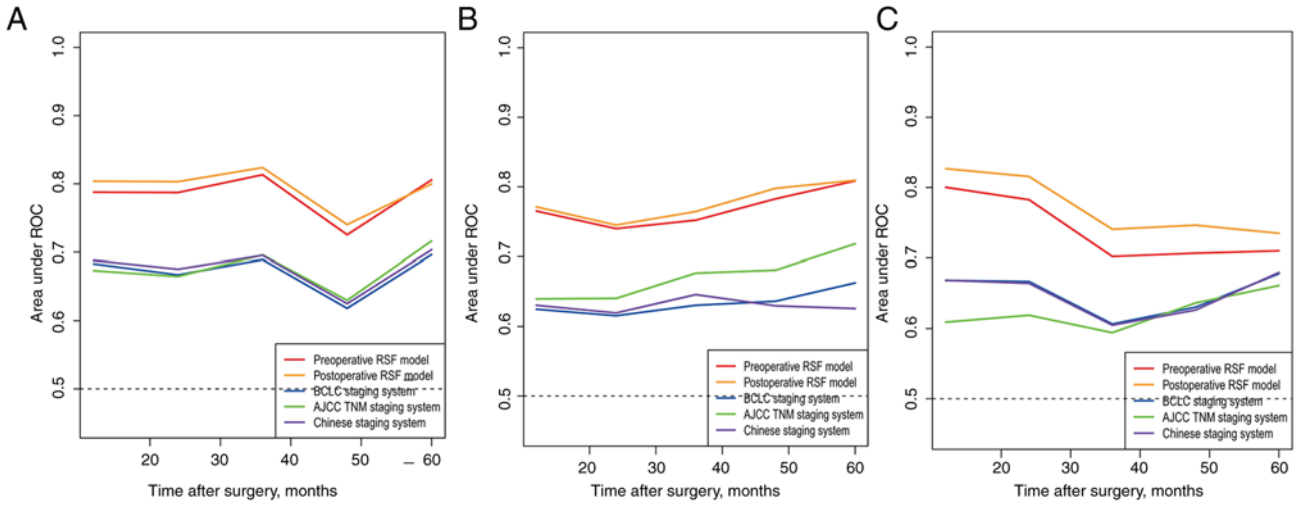

Figure 3. Time-dependent AUC of preoperative and postoperative of the RSF model in the training cohort, internal and external validation cohort. (A) training cohort, (B) internal validation cohort, and (C) external validation cohort.

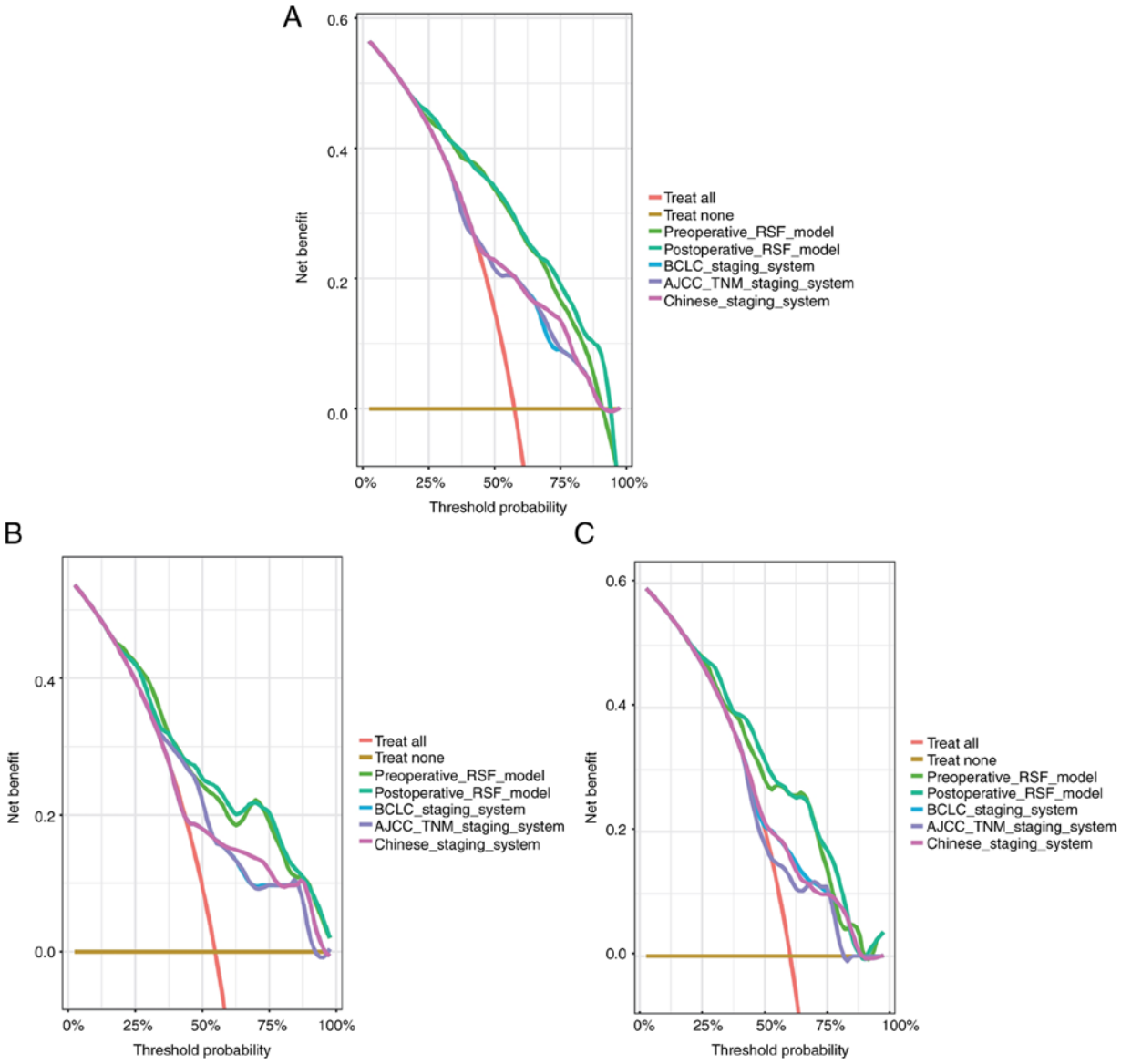

Figure 4. Comparison of decision curve analysis between the preoperative and postoperative RSF models and three other models (BCLC, AJCC, and Chinese staging system) in predicting recurrence of HCC. (A) Training cohort, (B) internal validation cohort, and (C) external validation cohort. RSF, random survival forests; AJCC TNM, American Joint Committee on Cancer Tumor-Node-Metastasis; BCLC, Barcelona Clinic Liver Cancer.

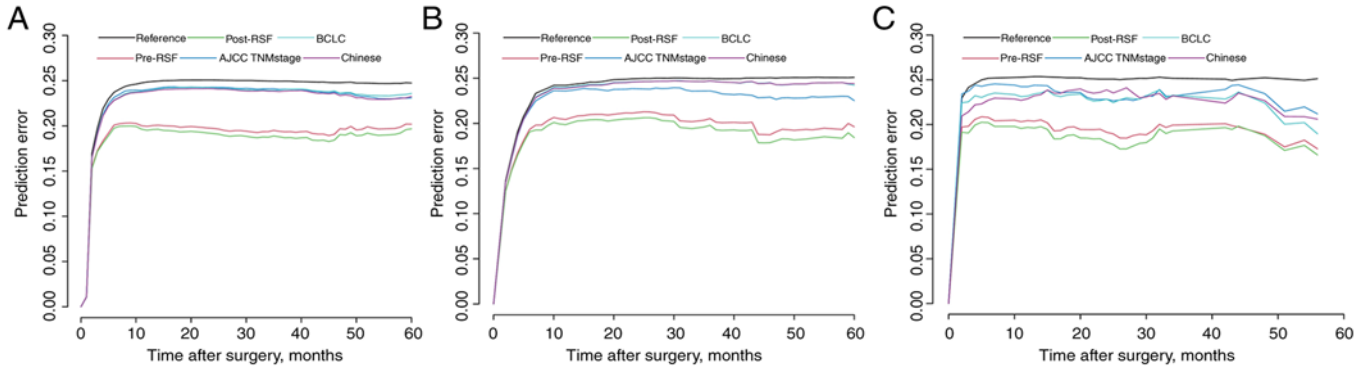

Figure 5. Comparison of prediction error curve between the preoperative and postoperative RSF model and three other models in predicting recurrence of HCC. (A) Training cohort, (B) internal validation cohort, and (C) external validation cohort. RSF, random survival forests; AJCC TNM, American Joint Committee on Cancer Tumor-Node-Metastasis; BCLC, Barcelona Clinic Liver Cancer.

shinyapps.io/post-operative_predict/) were developed for clinicians to use the RSF model (Figs. S1 and S2). This tool can output the risk index, risk groups, and the recurrence-free probability at 3, 6, 9, 12, 18, 24, 36, 48, and 60 months.

As shown in Fig. 8, both preoperative and postoperative RSF models could be used to re-stratify the patients with different recurrence risks at BCLC stage A (P<0.0001), BCLC stage B (P<0.0001), and BCLC stage C (P=0.0047, preoperative RSF model; P=0.0028, postoperative RSF model), respectively. In addition, both preoperative and postoperative RSF models could be used to distinguish the patients at the AJCC stage IB (P<0.0001), stage II (P<0.0001), stage IIIA (P<0.0001), and stage IIIB (P=0.015, preoperative RSF model; P=0.0039, postoperative RSF model), respectively (Fig. 9). Moreover, the preoperative and postoperative RSF models were effective in distinguishing the patients at stage IB of the Chinese staging system (P<0.0001), IIA (P<0.0001), IIB (P=0.049, preoperative RSF model; P=0.0042, postoperative RSF model), and IIIA (P=0.004, preoperative RSF model; P=0.0016, postoperative RSF model), respectively (Fig. 10).

Discussion

To date, a lack of reliable methods for the prediction of postoperative prognosis has been reported among patients with HCC (26). As a type of model superior to the CPH model, machine learning models offer a novel methodology based on their non-linear functions and can be used to improve the predictive efficiency for HCC as it considers all possible interactions between variables (27). In the present study, two RSF models with optimal preoperative and postoperative prediction for long-term prognosis following hepatectomy were constructed, and their predictive efficiency was evaluated using internal and external validations. The preoperative model contributed to the selection of treatment regimens for patients with huge HCC, while the postoperative model offered a more accurate and individualized prediction of prognosis following surgery.

To the best of our knowledge, this is the first study to validate a machine-learning model for predicting the recurrence of patients with huge HCC treated with curative resection. The data indicated that the RSF model was superior to the traditional staging models in model discrimination, clinical usefulness, and overall prediction efficiency. The primary advantage of the RSF model was attributed to the involved variables based on the non-linear risk function, without CPH-related assumptions. The preoperative and postoperative RSF models also indicated that the recurrence of huge HCC was primarily associated with tumor characteristics, such as MaVI, satellite nodules, tumor number, age, and higher AFP. According to previous studies, patients with MaVI may exhibit a decrease in liver function reserve, which serves as a high-risk factor for the recurrence of huge HCC (28,29), along with the satellite nodule (30). The satellite nodule was an independent risk factor for recurrence within 1 year following surgery (31). Studies have shown that the tumor number correlated with the recurrence of huge HCC (32,33). Xia *et al* (34) also reported that age was an independent risk factor for HCC early recurrence within 1 year of curative hepatectomy. Finally, a recent study indicated that a higher AFP level was also associated with a high 5-year recurrence rate of HCC (35). These studies further confirmed the association between tumor characteristics and recurrence prediction by the RSF modeling.

The preoperative and postoperative RSF models of the current study were able to re-stratify patients in the same traditional staging system stages and may therefore play a supplementary role to the traditional staging system. The preoperative RSF model, with a significantly improved predictive performance than the BCLC staging system, may serve as an additional tool for surgeons to identify high-risk patients prior to operation. It is important to note that the preoperative model can provide an important basis for the selection of the treatment regimen. The prognostic discrimination of the RSF model was able to accurately stratify patients into three prognostic subgroups as shown in Fig. 7. In clinical practice, TACE, sorafenib, or other alternative options are usually recommended to the patients with a poor RFS score prior to surgery and to those with poor tolerance to hepatectomy (36). Furthermore, the down-staging procedures may also be considered based on arterial chemoembolization, portal vein embolization (37), or even the associated liver partition with portal vein ligation for staged hepatectomy (38).

To date, there are still several follow-up procedures, which suggest that HCC patients present with a high possibility of recurrence (24). The postoperative RSF model contributes to the design of the follow-up procedures by surgeons, such as reduced interval for the follow-up and more high-end

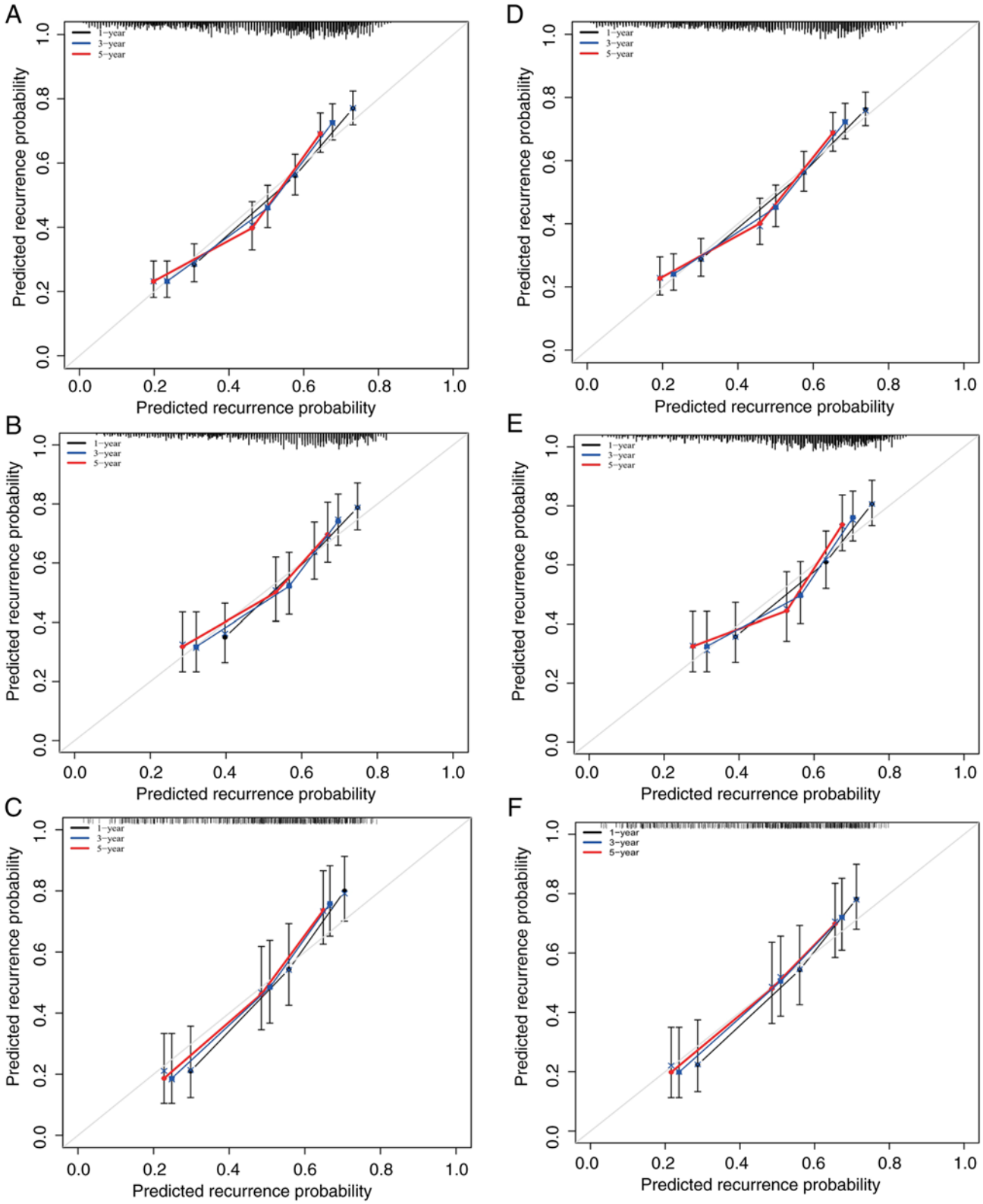

Figure 6. The calibration curves for predicting the 1-, 3-, and 5-year recurrence using the preoperative and postoperative random survival forests model. (A and D) Training cohort, (B and E) internal validation cohort, (C and F) external validation cohort.

imaging tests, as well as the utilization of adjuvant therapy for those with a high risk of recurrence (39). For the predictive efficiency of the models, the tdAUC and C-index of the postoperative RSF model were higher than those of the preoperative model; the prediction error curve and DCA also indicated that the postoperative model was more effective compared with that of the preoperative model. Additionally, the postoperative model may be superior to the preoperative model as it may include pathological variables, such as liver cirrhosis, tumor capsule, Edmondson-Steiner classification,

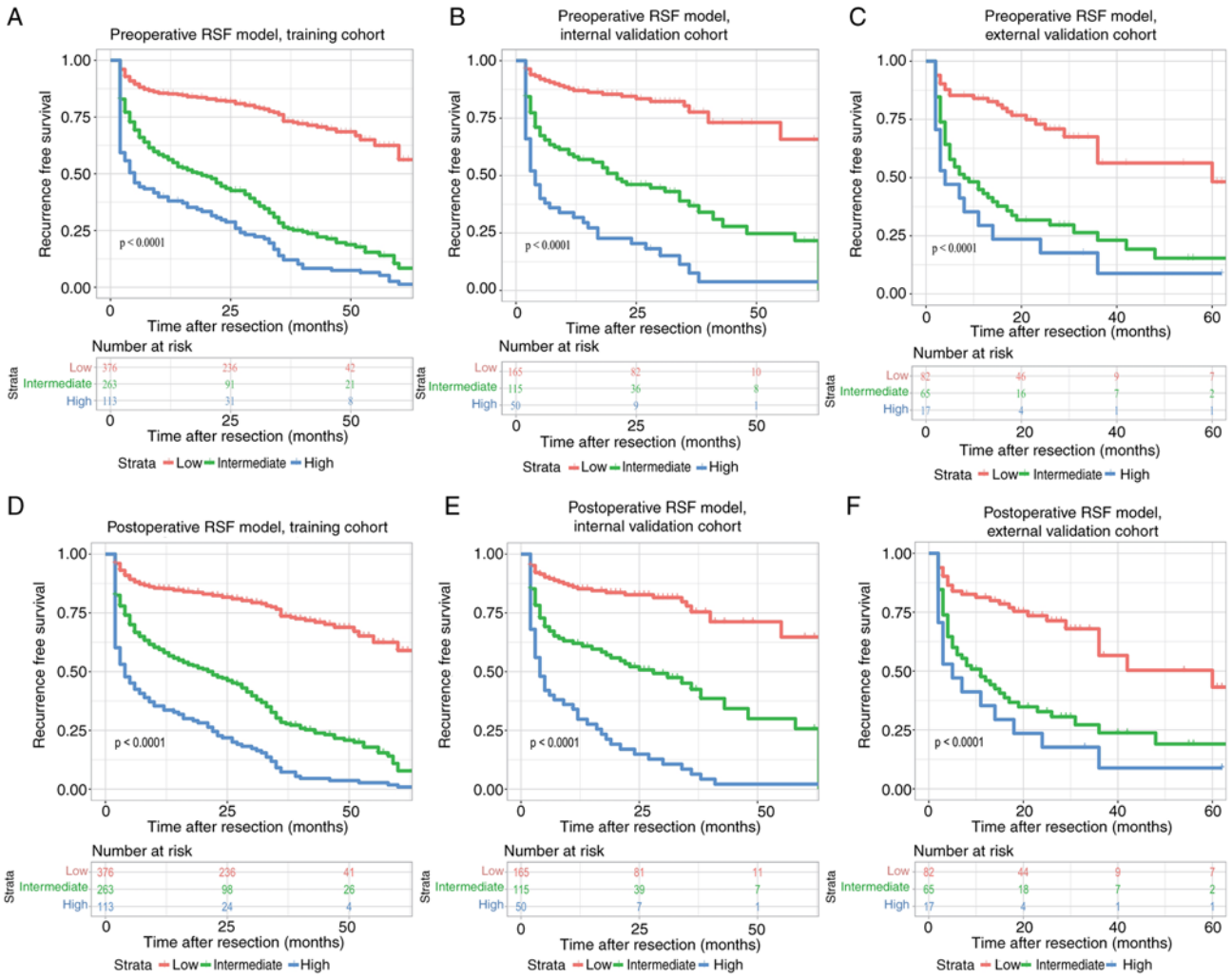

Figure 7. Kaplan-Meier plots for recurrence free survival rate of risk subgroups defined by the RSF model scores. (A) Preoperative RSF model, training cohort; (B) preoperative RSF model, internal validation cohort; (C) preoperative RSF model, external validation cohort; (D) postoperative RSF model, training Cohort; (E) postoperative RSF model, internal validation cohort; and (F) postoperative RSF model, external validation cohort. RSF, random survival forests.

MIV, as well as intraoperative blood transfusion. Patients with a huge HCC without tumor capsule were not likely to show a clear resection margin, leading to increased operative risks and a poorer prognosis following hepatectomy. Previously, a tumor size of ≥10 cm with no tumor capsule was shown to be an independent prognostic factor for poor OS and RFS after hepatectomy (40). Therefore, a complete tumor capsule for a huge HCC was an important factor for surgical safety and optimal long-term survival. Furthermore, an intact tumor capsule was considered a protective factor for recurrence, especially for those with huge tumors as it may inhibit local and vascular invasion (41,42). It has been well acknowledged that liver cirrhosis is related to the pathogenesis of HCC (43). In line with the previous data (44), the results of the present study confirmed that MVI was an independent risk factor for recurrence in huge HCC. Previously, Edmondson-Steiner grade had been reported as an independent predictive factor for recurrence (45). Wang *et al* (46) indicated that intraoperative transfusion of allogeneic blood was associated with a poorer clinical prognosis in patients with huge HCC who underwent radical hepatectomy. When the preoperative and postoperative models were used simultaneously, the preoperative model should be selected in the presence of indication of a poor prognosis for the preoperative model and the optimal prognosis based on the postoperative model, as the cost of shortening the follow-up interval was considerably lower than that of the cost of HCC recurrence. In the future, more prospective studies are required to distinguish the model with improved predictive power.

In addition, two inflammatory indices were included in the present study. According to VIMP analysis, PNLR and PLR were two important risk factors for the recurrence of huge HCC. According to previous studies, PNLR or PLR can be used as clinical indicators of the host inflammatory response and immune status, while an increasing PNLR or PLR is a strong predictor of poor survival in certain types of malignancies (47-50). It has been reported that a higher PNLR and PLR were correlated with a poorer prognosis among patients with HCC (48). Given that PNLR and PLR consist of a serum neutrophil count, a lymphocyte count, and a platelet count, a change in PNLR and PLR could be viewed as a relative increase in the number of neutrophils and platelet count, or a relative decrease in the number of lymphocytes. It has been demonstrated that neutrophils may promote tumor growth by

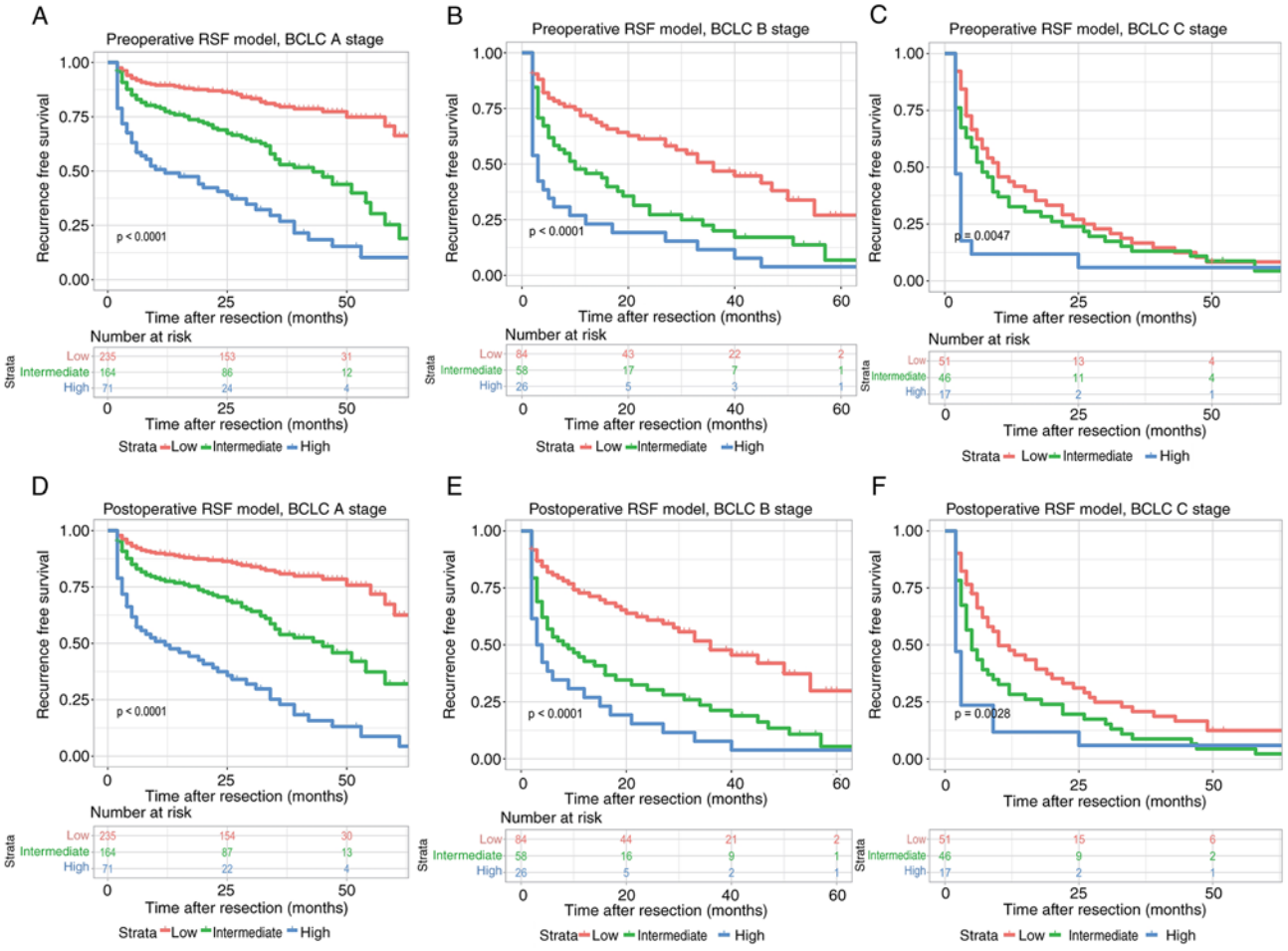

Figure 8. Kaplan-Meier plots for recurrence free survival rate of risk subgroups defined by the RSF model scores in the different BCLC stages. (A) Preoperative RSF model, BCLC A stage; (B) preoperative RSF model, BCLC B stage; (C) preoperative RSF model, BCLC C stage; (D) postoperative RSF model, BCLC A stage; (E) postoperative RSF model, BCLC B stage; and (F) postoperative RSF model, BCLC C stage. RSF, random survival forests; BCLC, Barcelona Clinic Liver Cancer.

increasing vascular endothelial growth factor, which serves as an important factor in promoting tumor angiogenesis (51). By contrast, several experimental studies have confirmed the relationship between the presence of malignancy and thrombocytosis (52-54). Following an increase in their number, the platelets can secrete several types of growth factors, which may stimulate the growth and proliferation of the tumor. Lastly, serving as one of the most important components of antitumor immunity, the reduction of the lymphocyte number was suggestive of abnormal immune mechanisms and a decline in antitumor immunity, which subsequently contributed to tumor invasion and metastasis (55). PNLR and PLR may reflect the tumor inflammation and immune status in the body; once this dynamic balance is interrupted, the tumor inflammatory response and antitumor inflammatory response will be destroyed. On this basis, normal immune function is impaired, thereby promoting metastasis and invasion of malignancies. It may help to explain why PNLR and PLR can be used to evaluate the probability of recurrence among patients with HCC. In the future, further studies are required to illustrate the mechanism underlying the association between PNLR, PLR, and the recurrence of huge HCC.

The present study has certain limitations. Firstly, this was a retrospective study involving a relatively small sample size, which may lead to unavoidable selection bias. Secondly, other variables that may be associated with the prognosis of patients with HCC (such as postoperative adjunctive therapies) were not evaluated in the present study. Thirdly, the model established was primarily based on two Chinese institutions of patients with HCC in hepatitis B virus-endemic areas. Additional cohorts from different geographic locations are required to validate our model to extend the results to patients with HCC of various etiologies. Finally, the present study was generated using data from patients who underwent radical resection, which may not be applicable for patients receiving other therapies, such as TACE and sorafenib. In the future, additional prospective studies involving long-term follow-up are essential to extend the feasibility of the established model.

In summary, the present study developed preoperative and postoperative RSF models based on machine learning algorithms for predicting the risk of huge HCC following resection. These two RSF models have accurate predictive ability and can play a supplementary role to the traditional staging system. Patients classified as high risk for recurrence based on the preoperative RSF model were recommended to receive non-surgical based treatment, or down-staging procedures followed by surgery, while those with low or moderate risks of recurrence on the preoperative model were recommended

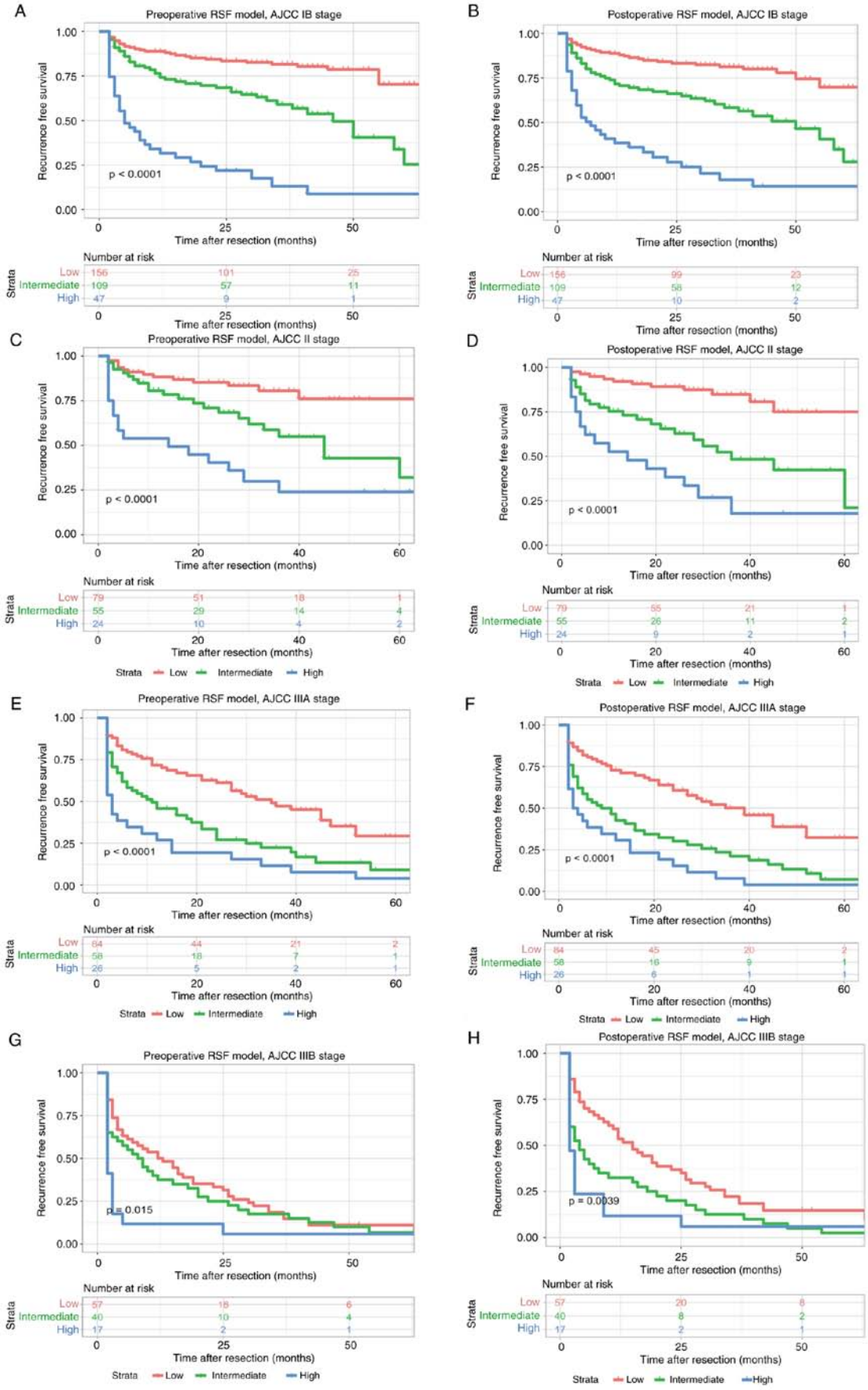

Figure 9. Kaplan-Meier plots for recurrence free survival rate of risk subgroups defined by the RSF model scores in different AJCC8th stage. (A) preoperative RSF model, AJCC8th IB stage; (B) postoperative RSF model, AJCC8th IB stage; (C) preoperative RSF model, AJCC8th II stage; (D) postoperative RSF model, AJCC8th II stage; (E) preoperative RSF model, AJCC8th IIIA stage; (F) postoperative RSF model, AJCC8th IIIA stage; (G) preoperative RSF model, AJCC8th IIIB stage; and (H) postoperative RSF model, AJCC8th IIIB stage. RSF, random survival forests; AJCC, American Joint Committee on Cancer; RSF, random survival forests; American Joint Committee on Cancer.

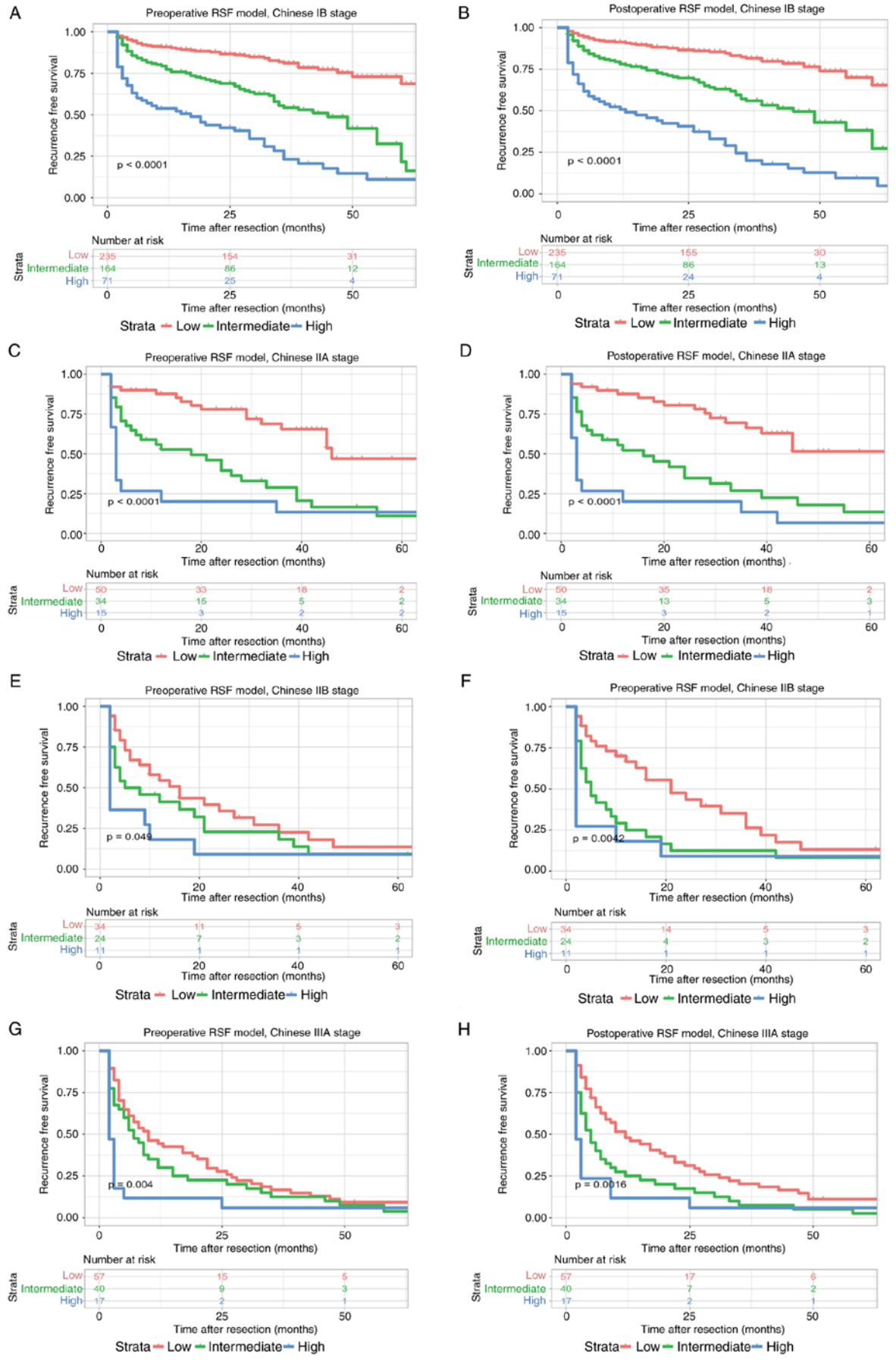

Figure 10. Kaplan-Meier plots for recurrence free survival rate of risk subgroups defined by RSF model scores in different Chinese stage. (A) Preoperative RSF model, Chinese IB stage; (B) postoperative RSF model, Chinese IB stage; (C) preoperative RSF model, Chinese IIA stage; (D) postoperative RSF model, Chinese IIA stage; (E) preoperative RSF model, Chinese IIB stage; (F) postoperative RSF model, Chinese IIB stage; (G) preoperative RSF model, Chinese IIIA stage; and (H) postoperative RSF model, Chinese IIIA stage. RSF, random survival forests.

to receive surgery. It was suggested that patients with high risk of recurrence based on the postoperative model should receive postoperative adjuvant therapy (such as TACE), while follow-up and monitoring were suggested for those with low and moderate risks.

Acknowledgements

Not applicable.

Funding

This study was supported by the Natural Science Foundation of Fujian Province (grant no. 2021J011283); and the Fuzhou Science and Technology Innovation Platform project (grant no. 2021-P-055).

Availability of data and materials

The datasets used and/or analyzed during the present study are available from the corresponding author on reasonable request.

Authors' contributions

HL and JL conceived the study. QZ, GF and TH, curated the data. QZ, GF, TH and GW performed the analysis. QZ, GF and TH confirm the authenticity of all the raw data. QZ, HL and JL wrote and reviewed the manuscript. All authors have read and approved the final manuscript.

Ethics approval and consent to participate

The study protocol used in the present study was approved by the Medical Ethics Committee of Mengchao Hepatobiliary Hospital of Fujian Medical University (approval no. 2022-027-01). Written informed consent for participation was not required for this study in accordance with the national legislation and the institutional requirements.

Patient consent for publication

Not applicable.

Competing interests

The authors declare that they have no competing interests.

References

1. Bray F, Ferlay J, Soerjomataram I, Siegel RL, Torre LA and Jemal A: Global cancer statistics 2018: GLOBOCAN estimates of incidence and mortality worldwide for 36 cancers in 185 countries. CA Cancer J Clin 68: 394-424, 2018.
2. Kim JM, Joh JW, Yi NJ, Choi GS, Kim K, Lee KW and Suh KS: Predicting hepatocellular carcinoma recurrence beyond milan criteria after liver resection for solitary hepatocellular carcinoma. J Gastrointest Surg 24: 2219-2227, 2020.
3. Nakagawa S, Wei L, Song WM, Higashi T, Ghoshal S, Kim RS, Bian CB, Yamada S, Sun X, Venkatesh A, *et al*: Molecular liver cancer prevention in cirrhosis by organ transcriptome analysis and lysophosphatidic acid pathway inhibition. Cancer Cell 30: 879-890, 2016.
4. Zhang H, Liu F, Wen N, Li B and Wei Y: Patterns, timing, and predictors of recurrence after laparoscopic liver resection for hepatocellular carcinoma: Results from a high-volume HPB center. Surg Endosc 36: 1215-1223, 2022.
5. Ruiz E, Pineau P, Flores C, Fernández R, Cano L, Cerapio JP, Casavilca-Zambrano S, Berrospi F, Chávez I, Roche B and Bertani S: A preoperative nomogram for predicting long-term survival after resection of large hepatocellular carcinoma (>10 cm). HPB (Oxford) 24: 192-201, 2022.
6. Hong SK, Lee KW, Hong SY, Suh S, Hong K, Han ES, Lee JM, Choi Y, Yi NJ and Suh KS: Efficacy of liver resection for single large hepatocellular carcinoma in child-pugh a cirrhosis: Analysis of a nationwide cancer registry database. Front Oncol 11: 674603, 2021.
7. Zhong NB, Lv GM and Chen ZH: Stereotactic body radiotherapy combined with transarterial chemoembolization for huge (≥10 cm) hepatocellular carcinomas: A clinical study. Mol Clin Oncol 2: 839-844, 2014.
8. Bai Y, Wu J, Zeng Y, Chen J, Wang S, Chen S, Qiu F, Zhou S, You S, Tian Y, *et al*: Nomogram for predicting long-term survival after synchronous resection for hepatocellular carcinoma and inferior vena cava tumor thrombosis: A multicenter retrospective study. J Oncol 2020: 3264079, 2020.
9. Chan AWH, Zhong J, Berhane S, Toyoda H, Cucchetti A, Shi K, Tada T, Chong CCN, Xiang BD, Li LQ, *et al*: Development of pre and post-operative models to predict early recurrence of hepatocellular carcinoma after surgical resection. J Hepatol 69: 1284-1293, 2018.
10. Mao S, Yu X, Shan Y, Fan R, Wu S and Lu C: Albumin-Bilirubin (ALBI) and monocyte to lymphocyte ratio (MLR)-based nomogram model to predict tumor recurrence of AFP-negative hepatocellular carcinoma. J Hepatocell Carcinoma 8: 1355-1365, 2021.
11. Camacho DM, Collins KM, Powers RK, Costello JC and Collins JJ: Next-generation machine learning for biological networks. Cell 173: 1581-1592, 2018.
12. Wang S and Summers RM: Machine learning and radiology. Med Image Anal 16: 933-951, 2012.
13. Rajkomar A, Dean J and Kohane I: Machine learning in medicine. N Engl J Med 380: 1347-1358, 2019.
14. Huang Y, Chen H, Zeng Y, Liu Z, Ma H and Liu J: Development and validation of a machine learning prognostic model for hepatocellular carcinoma recurrence after surgical resection. Front Oncol 10: 593741, 2020.
15. Knottnerus A and Tugwell P: STROBE-a checklist to strengthen the reporting of observational studies in epidemiology. J Clin Epidemiol 61: 323, 2008.
16. Marrero JA, Kulik LM, Sirlin CB, Zhu AX, Finn RS, Abecassis MM, Roberts LR and Heimbach JK: Diagnosis, staging, and management of hepatocellular carcinoma: 2018 practice guidance by the american association for the study of liver diseases. Hepatology 68: 723-750, 2018.
17. Yang P, Qiu J, Li J, Wu D, Wan X, Lau WY, Yuan Y and Shen F: Nomograms for pre- and postoperative prediction of long-term survival for patients who underwent hepatectomy for multiple hepatocellular carcinomas. Ann Surg 263: 778-786, 2016.
18. Taylor JM: Random survival forests. J Thorac Oncol 6: 1974-1975, 2011.
19. Ishwaran H, Kogalur UB, Blackstone EH and Lauer MSJTaoas: Random survival forests. The Annals of Applied Statistics 2: 841-860, 2008.
20. Royston P and Altman DG: External validation of a Cox prognostic model: Principles and methods. BMC Med Res Methodol 13: 33, 2013.
21. Mogensen UB, Ishwaran H and Gerds TA: Evaluating random forests for survival analysis using prediction error curves. J Stat Softw 50: 1-23, 2012.
22. Zhang XP, Wang K, Gao YZ, Wei XB, Lu CD, Chai ZT, Zhen ZJ, Li J, Yang DH, Zhou D, *et al*: Prognostic model for identifying candidates for hepatectomy among patients with hepatocellular carcinoma and hepatic vein invasion. Br J Surg 107: 865-877, 2020.
23. Chun YS, Pawlik TM and Vauthey JN: 8th edition of the AJCC cancer staging manual: Pancreas and hepatobiliary cancers. Ann Surg Oncol 25: 845-847, 2018.
24. European Association for the Study of the Liver. Electronic address: easloffice@easloffice.eu; European Association for the Study of the Liver: EASL clinical practice guidelines: Management of hepatocellular carcinoma. J Hepatol 69: 182-236, 2018.

25. Qiu G, Jin Z, Chen X and Huang J: Interpretation of guidelines for the diagnosis and treatment of primary liver cancer (2019 edition) in China. Glob Health Med 2: 306-311, 2020.
26. Li Y, Xia Y, Li J, Wu D, Wan X, Wang K, Wu M, Liu J, Lau WY and Shen F: Prognostic nomograms for pre- and postoperative predictions of long-term survival for patients who underwent liver resection for huge hepatocellular carcinoma. J Am Coll Surg 221: 962-974.e964, 2015.
27. Moncada-Torres A, van Maaren MC, Hendriks MP, Siesling S and Geleijnse G: Explainable machine learning can outperform Cox regression predictions and provide insights in breast cancer survival. Sci Rep 11: 6968, 2021.
28. Fang Q, Xie QS, Chen JM, Shan SL, Xie K, Geng XP and Liu FB: Long-term outcomes after hepatectomy of huge hepatocellular carcinoma: A single-center experience in China. Hepatobiliary Pancreat Dis Int 18: 532-537, 2019.
29. Li M, Zhao Y, Liu X, Zhang S, Jiang Y and Yang Z: Early risk warning system for distant metastasis of hepatitis B virus-associated hepatocellular carcinoma with portal vein tumor thrombus. Oncol Lett 19: 3249-3257, 2020.
30. Wang L, Liu Z, Liu X, Zeng Y and Liu J: The hepatectomy efficacy of huge hepatocellular carcinoma and its risk factors: A meta analysis. Medicine (Baltimore) 96: e9226, 2017.
31. Shin S, Kim TS, Lee JW, Ahn KS, Kim YH and Kang KJ: Is the anatomical resection necessary for single hepatocellular carcinoma smaller than 3 cm?: Single-center experience of liver resection for a small HCC. Ann Hepatobiliary Pancreat Surg 22: 326-334, 2018.
32. Wang XH, Liu QB, Xiang CL, Mao XH, Yang B, Li Q, Zhou QF, Li SQ, Zhou ZG and Chen MS: Multi-institutional validation of novel models for predicting the prognosis of patients with huge hepatocellular carcinoma. Int J Cancer 149: 127-138, 2021.
33. Dai T, Deng M, Ye L, Lin G, Liu R, Deng Y, Li R, Liu W, Li H, Yang Y, *et al*: Nomograms based on clinicopathological factors and inflammatory indicators for prediction of early and late recurrence of hepatocellular carcinoma after surgical resection for patients with chronic hepatitis B. Ann Transl Med 9: 12, 2021.
34. Xia W, Peng T, Guan R, Zhou Y, Zeng C, Lin Y, Wu Z and Tan H: Development of a novel prognostic nomogram for the early recurrence of liver cancer after curative hepatectomy. Ann Transl Med 9: 1541, 2021.
35. Ding HF, Zhang XF, Bagante F, Ratti F, Marques HP, Soubrane O, Lam V, Poultsides GA, Popescu I, Alexandrescu S, *et al*: Prediction of tumor recurrence by α-fetoprotein model after curative resection for hepatocellular carcinoma. Eur J Surg Oncol 47: 660-666, 2021.
36. Li H, Li S, Geng J, Zhao S, Tan K, Yang Z, Feng D and Liu L: Efficacy evaluation of the combination therapy of sorafenib and transarterial chemoembolization for unresectable HCC: A systematic review and meta-analysis of comparative studies. Ann Transl Med 8: 540, 2020.
37. Terasawa M, Allard MA, Golse N, Cunha AS, Cherqui D, Adam R, Saiura A and Vibert E: Sequential transcatheter arterial chemoembolization and portal vein embolization versus portal vein embolization alone before major hepatectomy for patients with large hepatocellular carcinoma: An intent-to-treat analysis. Surgery 167: 425-431, 2020.
38. Torres OJ, Vasques RR, Silva TH, Castelo-Branco ME and Torres CC: The ALPPS procedure for hepatocellular carcinoma larger than 10 centimeters. Int J Surg Case Rep 26: 113-117, 2016.
39. Ma L, Deng K, Zhang C, Li H, Luo Y, Yang Y, Li C, Li X, Geng Z and Xie C: nomograms for predicting hepatocellular carcinoma recurrence and overall postoperative patient survival. Front Oncol 12: 843589, 2022.
40. Zhang W, Zhang ZW, Zhang BX, Huang ZY, Zhang WG, Liang HF and Chen XP: Outcomes and prognostic factors of spontaneously ruptured hepatocellular carcinoma. J Gastrointest Surg 23: 1788-1800, 2019.
41. Arnaoutakis DJ, Mavros MN, Shen F, Alexandrescu S, Firoozmand A, Popescu I, Weiss M, Wolfgang CL, Choti MA and Pawlik TM: Recurrence patterns and prognostic factors in patients with hepatocellular carcinoma in noncirrhotic liver: A multi-institutional analysis. Ann Surg Oncol 21: 147-154, 2014.
42. Lee JI, Lee JW, Kim YS, Choi YA, Jeon YS and Cho SG: Analysis of survival in very early hepatocellular carcinoma after resection. J Clin Gastroenterol 45: 366-371, 2011.
43. Jiang CH, Yuan X, Li JF, Xie YF, Zhang AZ, Wang XL, Yang L, Liu CX, Liang WH, Pang LJ, *et al*: Bioinformatics-based screening of key genes for transformation of liver cirrhosis to hepatocellular carcinoma. J Transl Med 18: 40, 2020.
44. Zheng J, Shen S, Jiang L, Yan L, Yang J, Li B, Wen T, Wang W and Xu M: Outcomes of anterior approach major hepatectomy with diaphragmatic resection for single huge right lobe HCC with diaphragmatic invasion. Medicine (Baltimore) 97: e12194, 2018.
45. Zhou L, Rui JA, Zhou WX, Wang SB, Chen SG and Qu Q: Edmondson-Steiner grade: A crucial predictor of recurrence and survival in hepatocellular carcinoma without microvascular invasio. Pathol Res Pract 213: 824-830, 2017.
46. Wang JC, Hou JY, Chen JC, Xiang CL, Mao XH, Yang B, Li Q, Liu QB, Chen JB, Ye ZW, *et al*: Development and validation of prognostic nomograms for single large and huge hepatocellular carcinoma after curative resection. Eur J Cancer 155: 85-96, 2021.
47. Caram LJ, Calderon F, Masino E, Ardiles V, Mauro E, Haddad L, Pekolj J, Vicens J, Gadano A, de Santibañes E and de Santibañes M: Do changes in inflammatory markers predict hepatocellular carcinoma recurrence and survival after liver transplantation? Ann Hepatobiliary Pancreat Surg 26: 40-46, 2022.
48. Chen K, Zhan MX, Hu BS, Li Y, He X, Fu SR, Xin YJ and Lu LG: Combination of the neutrophil to lymphocyte ratio and the platelet to lymphocyte ratio as a useful predictor for recurrence following radiofrequency ablation of hepatocellular carcinoma. Oncol Lett 15: 315-323, 2018.
49. Ismael MN, Forde J, Milla E, Khan W and Cabrera R: Utility of inflammatory markers in predicting hepatocellular carcinoma survival after liver transplantation. Biomed Res Int 2019: 7284040, 2019.
50. Lin S, Hu S, Ran Y and Wu F: Neutrophil-to-lymphocyte ratio predicts prognosis of patients with hepatocellular carcinoma: A systematic review and meta-analysis. Transl Cancer Res 10: 1667-1678, 2021.
51. Kusumanto YH, Dam WA, Hospers GA, Meijer C and Mulder NH: Platelets and granulocytes, in particular the neutrophils, form important compartments for circulating vascular endothelial growth factor. Angiogenesis 6: 283-287, 2003.
52. An S, Shim H, Kim K, Kim B, Bang HJ, Do H, Lee HR and Kim Y: Pretreatment inflammatory markers predicting treatment outcomes in colorectal cancer. Ann Coloproctol 38: 97-108, 2022.
53. Lin MS, Gao MJ, Zhang DL, Li XY, Huang JX and Yu H: Prognostic significance of preoperative platelet-lymphocyte ratio in a Chinese cohort patient with colorectal cancer. Int J Clin Exp Pathol 10: 8686-8694, 2017.
54. Yoshida A, Sarian LO, Marangoni MJ, Firmano IC and Derchain SF: diagnostic value of the neutrophil/lymphocyte ratio, platelet/lymphocyte ratio, and thrombocytosis in the preoperative investigation of ovarian masses. Rev Bras Ginecol Obstet 42: 397-403, 2020.
55. Kitayama J, Yasuda K, Kawai K, Sunami E and Nagawa H: Circulating lymphocyte number has a positive association with tumor response in neoadjuvant chemoradiotherapy for advanced rectal cancer. Radiat Oncol 5: 47, 2010.